A Letters Journal Exploring the Frontiers of Physics

January 2011

EPL, **93** (2011) 18003
doi: 10.1209/0295-5075/93/18003

www.epljournal.org

Coupled multimode optomechanics in the microwave regime

Georg Heinrich and Florian Marquardt

Arnold Sommerfeld Center for Theoretical Physics, Center for NanoScience and Department of Physics, Ludwig-Maximilians-Universität München - Theresienstr. 37, D-80333 München, Germany, EU and Institut für Theoretische Physik, Universität Erlangen-Nürnberg - Staudtstr. 7, 91058 Erlangen, Germany, EU

received 18 May 2010; accepted in final form 23 December 2010
published online 1 February 2011

PACS 85.85.+j – Micro- and nano-electromechanical systems (MEMS/NEMS) and devices
PACS 84.40.Dc – Microwave circuits
PACS 42.50.Dv – Quantum state engineering and measurements

Abstract – The motion of micro- and nanomechanical resonators can be coupled to electromagnetic fields. This allows one to explore the mutual interaction and introduces new means to manipulate and control both light and mechanical motion. Such optomechanical systems have recently been implemented in nanoelectromechanical systems involving a nanomechanical beam coupled to a superconducting microwave resonator. Here, we propose optomechanical systems that involve multiple, coupled microwave resonators. In contrast to similar systems in the optical realm, the coupling frequency governing photon exchange between microwave modes is naturally comparable to typical mechanical frequencies. For instance this enables new ways to manipulate the microwave field, such as mechanically driving coherent photon dynamics between different modes. In particular we investigate two setups where the electromagnetic field is coupled either linearly or quadratically to the displacement of a nanomechanical beam. The latter scheme allows one to perform QND Fock state detection. For experimentally realistic parameters we predict the possibility to measure an individual quantum jump from the mechanical ground state to the first excited state.

Introduction. – Significant interest in the interaction and dynamics of systems comprising micro- and nanomechanical resonators coupled to electromagnetic fields, as well as the prospect to eventually measure and control the quantum regime of mechanical motion, has stimulated the rapidly evolving field of optomechanics (see [1] for a recent review). In the standard setup, the light field, stored inside an optical cavity, exerts a radiation pressure force on a movable end-mirror whose motion changes the cavity frequency and thus acts back on the photon dynamics. This way, the photon number inside the optical mode is linearly coupled to the displacement of a mechanical object. Beyond the standard approach, new developments have introduced optical setups with multiple coupled light and vibrational modes pointing the way towards integrated optomechanical circuits [2–6]. These systems allow one to study elaborate interactions between mechanical motion and light such as mechanically driven coherent photon dynamics that introduces the whole realm of driven two- and multi-level systems to the field of optomechanics [7]. Coupled multimode setups furthermore allow one to increase measurement sensitivity [8] and enable fundamentally different coupling schemes. Accordingly, recent experiments achieved coupling the photon number to the square and quadruple of mechanical displacement [2,9]. Such different coupling schemes are needed, for instance, to afford quantum non-demolition (QND) Fock state detection of a mechanical resonator [2,10–12].

Besides optics, recent progress has made it possible to realize optomechanical systems in the microwave regime [13,14]. In this case the optical cavity is replaced by a superconducting microwave resonator whose central conductor capacitively couples to the motion of a nanomechanical beam. This optomechanical approach constitutes a new path to perform on-chip experiments measuring and manipulating nanomechanical motion that adds to electrical concepts using single electron transistors [15–17], superconducting quantum interference devices [18,19], driven RF circuits [20] or a Cooper-pair box [21,22]. One advantage of on-chip optomechanics is to use standard bulk refrigerator techniques in addition to laser-cooling schemes [23,24]. This recently enabled cooling a single vibrational mode close to the quantum-mechanical ground state [25]. Furthermore, nonlinear

circuit elements can be integrated. This afforded ultrasensitive displacement measurements with measurement imprecision below that at the standard quantum limit [26].

Here we go beyond single mode systems, that have been considered for microwave optomechanics so far, and propose setups with coupled microwave resonators. As we show, the microwave regime is especially promising for coupled multimode optomechanics as it offers explicit advantages compared to the optical realm. In particular, it allows one to conveniently access a new regime where the coupling frequency between microwave modes is comparable to mechanical frequencies. This has several implications both for the classical and the prospective quantum regime. In addition, on-chip fabrication and the use of bulk refrigerator techniques are further advantages that directly relate to the prospects to perform quantum measurements of mechanical motion.

Accordingly, we start with a two-resonators setup with linear mechanical coupling. The derivation of the Hamiltonian allows one to discuss the feasibility of a new regime for optomechanics. Selecting one example that focus on the domain of classical mechanical motion that is accessible in experiments at present, we demonstrate how this new regime, for instance, allows one to manipulate the microwave field in terms of mechanical driving. For simplicity, here we consider two-resonator setups but our findings directly translate to larger systems. In the last part of this letter we present a multimode microwave scheme that allows coupling to the square of displacement. As an example regarding prospective quantum measurements we discuss QND Fock state detection using this device.

Two-resonators setup with linear mechanical coupling. – We consider the coplanar device geometries depicted in fig. 1(a) with two identical superconducting microwave resonators a_L, a_R. The central conductors of a_L and a_R are assumed to adjoin for a length d_g that is much smaller than the total wave guides' length d (fig. 1(b)). A nanomechanical beam, connected to the ground plane, is placed at the other end of a_L (fig. 1(c)).

Hamiltonian. Heuristically, the form of the Hamiltonian for the system depicted in fig. 1 can be guessed. Considering two microwave modes with frequency ω_L, ω_R and photon number operator $a_L^\dagger a_L$, $a_R^\dagger a_R$ in the left and right resonator, respectively, its general structure reads

$$\mathcal{H} = \hbar\left(\omega_L - \epsilon x\right) a_L^\dagger a_L + \hbar\omega_R a_R^\dagger a_R + \hbar g\left(a_L^\dagger a_R + a_R^\dagger a_L\right). \quad (1)$$

Due to the resonators' alignment there is a tunnel coupling of photons between the two modes described in terms of a coupling frequency g. Furthermore, via the left resonator's capacitance, the motion of the mechanical beam x shifts its resonance frequency where $\epsilon = -\partial\omega/\partial x$ is the optomechanical frequency pull per displacement. For an explicit discussion of the microwave regime, however, we have to derive eq. (1). For instance, this will yield the parameters' dependence.

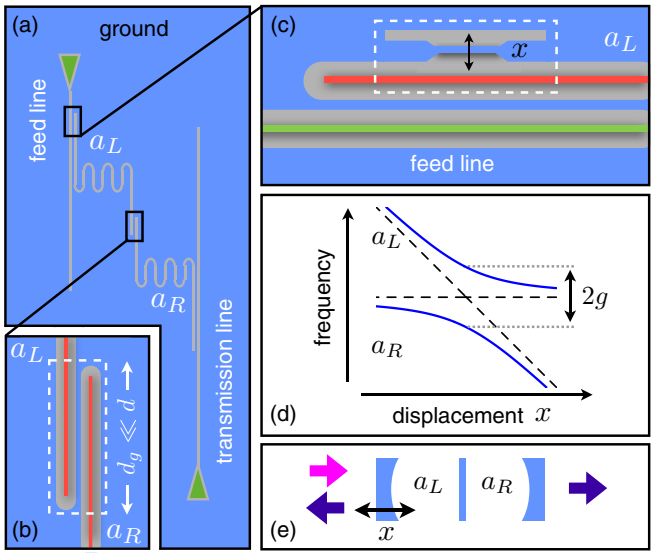

Fig. 1: (Colour on-line) Schematic device geometry for two superconducting microwave resonators a_L, a_R with a nanomechanical beam coupled to a_L. (a) The two resonators (each of length d) are coupled to external feed and transmission lines (green). (b) The central conductors of a_L and a_R (red) capacitively couple due to a small region of length d_g where the resonators adjoin. (c) At the other end of a_L a small mechanical beam, connected to ground (blue), is placed. Its displacement x affects the line capacitance of resonator a_L changing its resonance frequency. (d) System's resonance frequency as function of displacement: the beam's displacement x linearly changes the bare mode frequency of a_L while the one of a_R is unaffected (dashed). Due to the coupling g between modes there is an avoided crossing $2g$ in the eigenfrequencies (blue). (e) Analogous optical setup: a static, dielectic membrane, placed inside a cavity with a movable mirror, couples two separate optical modes a_L, a_R.

Rigorously, the Hamiltonian of an electric circuit can be derived from its Lagrangian (see, for instance, [27]). The latter can conveniently be expressed in terms of a flux variable $\phi(x,t) \equiv \int_{-\infty}^{t} \mathrm{d}\tau\, V(x,\tau)$, where $V(x,t) = \partial_t \phi(x,t)$ is the voltage at position x and time t. Without the nanomechanical beam, the circuit diagram looks as depicted in fig. 2. As the length d_g of the region where a_L and a_R adjoin is much smaller than the resonators' length d, the capacitive coupling between both central conductors can be considered in terms of a constant, total capacitance G. Given the circuit diagram, each node defines an equation of motion for the flux at that position. This allows to derive the corresponding Lagrangian [27]. For fig. 2 we find $\mathcal{L} = \mathcal{L}_L + \mathcal{L}_R + \frac{G}{d}(\sum_k \dot\phi_{R,k} - \sum_k \dot\phi_{L,k})^2$, where $\phi_{L,k}$, $\phi_{R,k}$ refer to the uncoupled ($G = 0$) normal modes of the flux in the left and right resonator, respectively; and $\mathcal{L}_j = \sum_k [\frac{c}{2}\dot\phi_{j,k}^2 + \frac{1}{2l}\left(\frac{k\pi}{d}\right)^2 \phi_{j,k}^2]$ $(j = L, R)$ describes the corresponding Lagrangian for separate resonators, each with line inductance l and line capacitance c [28]. To transform

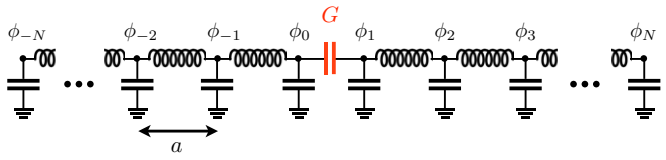

Fig. 2: (Colour on-line) Discretized circuit diagram for the system depicted in fig. 1 without nanomechanical beam. The flux variable $\phi(x,t)$ is discretized as $\phi_n(t)$ at node $x = na$. The two central conductors are coupled via a total capacitance G.

to the Hamiltonian, we consider the canonically conjugated momentum $\pi_{L[R],k} = \partial L/\partial\dot{\phi}_{L[R],k}$. For $G/d \ll c$ (see discussion below), the expression for $\pi_{L[R],k}$ simplifies to $\pi_{L[R],k} = c\dot{\phi}_{L[R],k}$. In the following we will restrict to a single mode in each resonator ($k = 1$), and drop the label referring to the mode index. Then, the Legendre transformation transforms $\mathcal{L}_L$, $\mathcal{L}_R$ into two harmonic oscillators of frequency ω_L and ω_R. For the coupling we consider $(\dot{\phi}_R - \dot{\phi}_L)^2$ with $\dot{\phi}_{L[R]} = \pi_{L[R]}/c = i\sqrt{\hbar\omega_{L[R]}/2c}(a^\dagger_{L[R]} - a_{L[R]})$, see [28]. As the microwave frequency is by far the fastest time scale involved in the system, we can use a rotating wave approximation and find for the Hamiltonian,

$$\mathcal{H} = \hbar\omega_L\left(1 - \frac{G}{dc}\right)a_L^\dagger a_L + \hbar\omega_R\left(1 - \frac{G}{dc}\right)a_R^\dagger a_R + \hbar\sqrt{\omega_L\omega_R}\frac{G}{dc}\left(a_L^\dagger a_R + a_R^\dagger a_L\right), \tag{2}$$

where we neglected the vacuum energy. We note that the frequencies ω_L, ω_R, originally defined for uncoupled modes, are lowered by a constant value. This shift can be neglected by simply redefining the resonators' frequencies. More important is the coupling between modes. From our derivation we can read off its frequency

$$g = \sqrt{\omega_L\omega_R}\frac{G}{dc}. \tag{3}$$

Finally we take into account the nanomechanical beam. For the resonator a_L in fig. 1, the beam's motion changes the capacitance between the central conductor and the ground plane. We find the optomechanical frequency pull per displacement $\epsilon_k = -\partial\omega_k/\partial x$ from the resonance frequency of a microwave resonator, $\omega_k = k\pi/d\sqrt{lc}$. This yields $\epsilon_k = (\partial C_b/\partial x)\cdot Z\cdot\omega_k^2/(2\pi k)$, where C_b denotes the total capacitance between the central conductor and the beam. $Z = \sqrt{l/c}$ is the line impedance.

Altogether this yields the Hamiltonian whose form was already stated in eq. (1). We note that according to eq. (3) with $\omega_L(x)$, the coupling frequency g in principle depends on displacement x. However, for typical parameters the dependence is negligible and g can be considered to be constant. The resonance frequency of eq. (1) is depicted in fig. 1(d).

Coupling frequency comparable to the mechanical frequency ($g \simeq \Omega$). Given eq. (3), the coupling frequency between the two resonator modes reads $g/\omega_0 = (c_g/c)\cdot(d_g/d)$, where we defined the coupling line capacitance $c_g = G/d_g$ along the length of the coupling region d_g. In general, c_g will be much smaller than the line capacitance between each central conductor and the ground plane c: first of all, the distance between the two central conductors is significantly larger than the distance between a single conductor and the adjacent ground plane. Second, the capacitance between the central strip lines is shielded by the grounded region in between. Here we crudely assume $c_g/c = 10^{-2}$. For d in the cm range and $d_g \simeq 0.1\,\mathrm{mm}$ (d_g is chosen such that a several $10\,\mu$m long nanomechanical beam can be fabricated in between the region where the resonators align), we have $d_g/d = 10^{-2}$ and the coupling between modes is $g/\omega_0 = 10^{-4}$, where ω_0 will be in the GHz range. Common eigenfrequencies of nanomechanical beams are $\Omega = 100\,\mathrm{kHz}$–$10\,\mathrm{MHz}$. Hence, due to their much smaller photon frequency, coupled multimode optomechanical systems in the microwave regime naturally possess coupling frequencies in the range of typical mechanical frequencies ($g \simeq \Omega$). The relevance of this regime for instance to realize all kinds of driven two- and multi-level photon dynamics in optomechanical systems has been pointed out in [7].

Mechanically driven photon dynamics. As an example to emphasize the characteristics of coupled optomechanical systems in the microwave regime and to demonstrate implications of $g \simeq \Omega$ even in the presently accessible regime of classic mechanical motion, we will discuss how the microwave field in the setup of fig. 1 can be manipulated in terms of mechanical driving (see [29] for a universal mechanical actuation scheme). Experimentally, the impact can be most easily observed in terms of the transmission spectrum. We assume the left resonator a_L to be driven at frequency ω_L via the feed line, while the transmission down the transmission line is recorded. We consider the coupling of the left (right) resonator to the feed (transmission) line in terms of the resonators' decay rate κ. Given the Hamiltonian (1), using input/output theory, the equation of motion for the averaged fields $\alpha_L = \langle a_L\rangle$, $\alpha_R = \langle a_R\rangle$ read

$$\begin{aligned}\frac{\mathrm{d}}{\mathrm{d}t}\alpha_L &= \frac{1}{i}\left(-\epsilon x(t)\alpha_L + g\alpha_R\right) - \frac{\kappa}{2}\alpha_L - \sqrt{\kappa}b_L^{in}(t),\\ \frac{\mathrm{d}}{\mathrm{d}t}\alpha_R &= \frac{1}{i}g\alpha_L - \frac{\kappa}{2}\alpha_R,\end{aligned} \tag{4}$$

where $b_L^{in}(t) = e^{-i\Delta_L t}b^{in}$ describes the electromagnetic drive along the feed line with amplitude b^{in} and frequency ω_L. Here we used a rotating frame with laser detuning from resonance $\Delta_L = \omega_L - \omega_0$. The transmission $T(t) = \kappa\langle a_R^\dagger(t)a_R(t)\rangle/(b^{in})^2$ can be expressed as

$$T(t) = \kappa^2\left|\int_{-\infty}^{t} G(t,t')e^{-i\Delta_L t' - (\kappa/2)(t-t')}\,\mathrm{d}t'\right|^2, \tag{5}$$

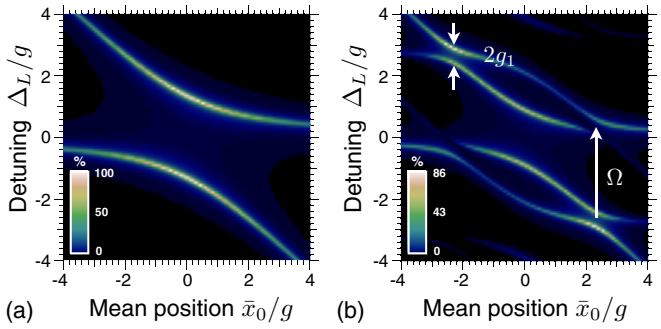

Fig. 3: (Colour on-line) Transmission spectrum for the setup depicted in fig. 1 for resonators' decay rate $\kappa = 0.1g$: density plot for the time-averaged transmission depending on mean mechanical displacement $\bar{x}_0 = \epsilon x_0$, and frequency detuning $\Delta_L = \omega_L - \omega_0$ of the feed line's microwave drive at ω_L (ω_0 denotes the left mode's bare frequency for $x = 0$). (a) Without mechanical drive ($x(t) = x_0$); the spectrum is given by the resonance frequency depicted in fig. 1(d). (b) For mechanical driving ($x(t) = A\cos(\Omega t) + x_0$) with amplitude $\bar{A} = \epsilon A = 1.5\Omega$ and frequency $\Omega = 3g$; mechanical sidebands displaced by Ω appear and intersect the original photon branches where, due to mechanically driven Rabi dynamics, high transmission and additional anticrossings arise. The gap $2g_1$ is determined by the Bessel function J_1 according to $2g_1 = 2gJ_1(\bar{A}/\Omega)$.

where the phase comprises the feed line's drive and resonators' decay, while the Green's function $G(t, t')$ describes the amplitude for a photon to enter the left resonator's mode a_L at time t' and to be found in the right one a_R later at time t.

We take into account two scenarios: first, the beam is at rest given a constant displacement $x(t) = x_0$; second, the beam is mechanically driven to oscillate with amplitude A and frequency Ω around the mean position x_0, $x(t) = x_0 + A\cos(\Omega t)$. Figure 3(a) shows numerical results of the transmission spectrum without mechanical driving. The spectrum corresponds to the system's resonance frequency depicted in fig. 1(d) where the resonance width is set by the resonators' decay rate κ. In contrast, fig. 3(b) shows the transmission including mechanical driving with $\Omega = 3g$, *i.e.* $g \simeq \Omega$ being characteristic for coupled microwave optomechanics. In this case, the mechanics moves on a time scale that is comparable to the one governing photon exchange between modes. This results in new, nonequilibrium photon dynamics that goes beyond the usual adiabatic case $g \gg \Omega$.

To understand the main features of fig. 3(b) we note that, in general, two processes are involved to observe transmission, see (5): first, the left resonator a_L must be excited by the electromagnetic drive $b_L^{in}(t) = e^{-i\Delta_L t} b^{in}$; second, the internal dynamics must be able to transfer photons from a_L to a_R. From (4) the solution $G(t, t')$ can be found to be

$$G(t, t') = \tilde{\alpha}_R(t, t') e^{-i\phi(t')}, \tag{6}$$

where $\phi(t') = (\bar{A}/\Omega)\sin(\Omega t')$ and $\tilde{\alpha}_R(t, t')$ is a solution to the driven two-state problem

$$\frac{\mathrm{d}}{\mathrm{d}t}\begin{pmatrix}\tilde{\alpha}_L \\ \tilde{\alpha}_R\end{pmatrix} = \frac{1}{i}\begin{pmatrix}-\bar{x}_0 & g e^{-i\phi(t)} \\ g e^{+i\phi(t)} & 0\end{pmatrix}\begin{pmatrix}\tilde{\alpha}_L \\ \tilde{\alpha}_R\end{pmatrix}, \tag{7}$$

with $t \geqslant t'$ and initial condition $\tilde{\alpha}_L(t', t') = 1$, $\tilde{\alpha}_R(t', t') = 0$. Note that we expressed displacement in terms of frequency; $\bar{A} = \epsilon A$, $\bar{x}_0 = \epsilon x_0$. For $\bar{A} \neq 0$, in addition to the electromagnetic drive (see $e^{-i\Delta t'}$ in (5)), the mechanical driving can excite a_L in terms of multiples of the mechanical frequency $m\Omega$. This mechanical excitation is described by the phase factor $e^{-i\phi(t')} = \sum_m J_m(\bar{A}/\Omega) e^{-im\Omega t'}$ in (6) and leads to mechanical sidebands in the spectrum (cf. fig. 3(b)). Note that the individual process $m\Omega$ is described by a Bessel function $J_m(\bar{A}/\Omega)$ and can be tuned by the driving strength. Beyond the modified excitation, the driving significantly changes the internal dynamics of the microwave fields, see eq. (7). In particular the mechanical motion can initiate mechanically driven Rabi dynamics exchanging photons between a_L and a_R that leads to high transmission if the mechanical drive at Ω is in resonance with the modes' frequency difference. For sufficiently strong driving, the mechanically assisted process leads to additional anticrossings in the spectrum resembling Autler-Townes splittings known from quantum optics (see marker in fig. 3(b)). From eq. (7) we find that the spacing of this first additional splitting scales according to $2gJ_1(\bar{A}/\Omega)$ and can likewise be tuned by the mechanical driving strength. All this illustrates how, due to $g \simeq \Omega$, the microwave field can extensively be manipulated by mechanical motion in terms of mechanically driven coherent photon dynamics.

Coupling to the square of displacement. – We present a modified scheme comprising coupled microwave resonators that allows one to couple the photon number to the *square* of mechanical displacement (fig. 4(a),(b)). In contrast to the setup in fig. 1, here the nanomechanical beam is placed in the region *between* the two resonators, such that its motion affects both simultaneously (fig. 4(b)). According to our previous results, the Hamiltonian reads

$$\begin{aligned} H \;=\; & \hbar\left(\omega_0 - \epsilon x\right) a_L^\dagger a_L + \hbar\left(\omega_0 + \epsilon x\right) a_R^\dagger a_R \\ & + \hbar g\left(a_L^\dagger a_R + a_R^\dagger a_L\right), \end{aligned} \tag{8}$$

where $g = \omega_0 c_g d_g / cd$, see (3) and (1).

Figure 4(c) illustrates the system's resonance frequency $\omega_\pm(x) = \omega_0 \pm \sqrt{g^2 + (\epsilon x)^2}$ as a function of displacement. Naturally all the characteristics of coupled multimode optomechanics in the microwave regime, that have been discussed, apply. In particular, the hyperbola-shaped avoided level crossing allows one to realize Landau-Zener-Stueckelberg dynamics in microwave fields [7].

At the extrema of $\omega_\pm(x)$ the Hamiltonian allows an exclusive coupling to the square of mechanical displacement x^2. In principle, such a coupling allows one to

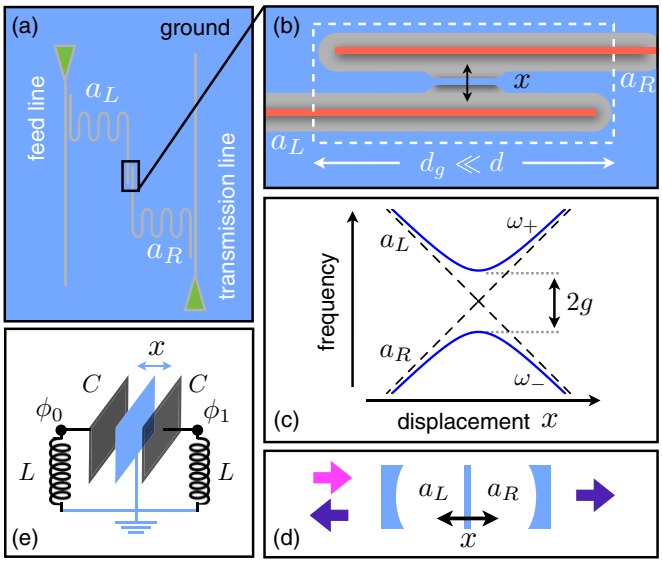

Fig. 4: (Colour on-line) Schematic device geometry for two microwave resonators a_L, a_R with a nanomechanical device coupled to *both* of them. (a) Two stripline resonators (each of length d) are coupled to external feed and transmission lines (green). The central conductors of a_L, a_R (red) are capacitively coupled in a small region of length d_g where the wave guides adjoin. (b) Between the two resonators a small mechanical beam, connected to ground (blue), is placed. Its displacement x affects the line capacitance of both, a_L and a_R. (c) System's resonance frequency as function of displacement: the beam's displacement linearly changes the bare modes' frequency of a_L and a_R (dashed). Due to the coupling g between the resonators, there is an avoided crossing $2g$ in the eigenfrequencies $\omega_\pm$ (blue). (d) Analogous optical setup with a movable dielectric membrane placed in the middle of a cavity [2]. (e) Schematic realization with two microwave LC circuits where a central plate is grounded and resonates against two others that build the LC circuits. In the notation of fig. 2 we get for the coupling frequency $g = \omega_{LC} G/C$ with $\omega_{LC} = 1/\sqrt{LC}$.

perform QND Fock state detection and to observe quantum jumps of a mechanical resonator [10,11]. Indeed, the Hamiltonian (8) corresponds to the one found for an optical setup (see fig. 4(d)), that generated a lot of interest in this regard [2,12]. Focussing on one microwave mode with annihilation operator a, we expand the resonance frequency $\omega_+(x)$ around x_0. For $x_0 = 0$ the linear contribution vanishes and the Hamiltonian reads $H = \hbar(\omega_+(0) + \frac{1}{2}\omega_+''(0)x_{zp}^2[b^\dagger + b]^2)a^\dagger a + \hbar\Omega b^\dagger b$, where we considered the phonon number operator $n = b^\dagger b$ and quantized $(x - x_0)$ using the mechanical beam's displacement operator $\hat{x} = x_{zp}\left(b^\dagger + b\right)$. The zero-point displacement $x_{zp} = \sqrt{\hbar/2m\Omega}$ is determined by the mechanical mass m and frequency Ω. If we do a rotating wave approximation (RWA), neglecting the non-commuting terms $(b^\dagger + b)^2 \simeq 2n + 1$, we see that $[H, n] = 0$.

Beyond this general principle, a rigorous analysis for real experiments must consider existing non-commuting terms, the thermal environment as well as detection limits due to shot-noise or measurement added fluctuations. This is very different to the optical realm. In addition, we have modified parameters such as ultra-light–weight mechanics, microwave frequencies or the modes' coupling found above.

Fock state detection in the MW regime. For a realistic estimate on the prospects to perform Fock state detection, we calculate the signal-to-noise ratio to detect mechanical quantum jumps. We consider an experimental scheme in analogy to the one proposed for the optical setup [2]. Accordingly, the mechanics is cooled to the quantum-mechanical ground state [23,25]. After switching off the cooling, the phonon number n is measured via the frequency of the microwave mode. To detect a quantum jump from $n = 0$ to $n = 1$, the frequency shift per phonon $\Delta\omega = \omega_+''(0)x_{zp}^2$, where $\omega_+''(0) = \epsilon^2/g$, must be resolved within the lifetime of the phonon ground state $\tau^{(0)}$. Given the imprecision of the frequency measurement in terms of the angular frequency noise power spectral density $S_{\omega\omega}$ (in units of $\mathrm{s}^{-2}/\mathrm{Hz}$), the signal-to-noise ratio reads

$$\Sigma = (\Delta\omega)^2 \tau^{(0)}/S_{\omega\omega}. \tag{9}$$

In contrast to the optical regime, where shot-noise–limited frequency measurements are routinely achieved, microwave setups in general suffer from amplifier noise adding n_{add} quanta of noise beyond the fundamental shot-noise limit in a Pound-Drever-Hall scheme (see [30]), such that $S_{\omega\omega} = (n_{add} + 1/2)\kappa^2\hbar\omega_c/16P_{in}$. P_{in} denotes the incident power and ω_c is the resonance frequency of the microwave mode. While commercially available systems add a significant amount of noise, a new Josephson parametric amplifier achieved $n_{add} < 1/2$ [31]. This technique has already been used for displacement measurements in a microwave optomechanical system with $n_{add} = 1.3$ [26].

Finally, we have to determine $\tau^{(0)}$. On the one hand, the ground state's total lifetime $\tau^{(0)} = 1/(\tau_T^{-1} + \tau_{RWA}^{-1} + \tau_{lin}^{-1})$ is set by the thermal lifetime $\tau_T = \hbar Q/k_B T$ via the mechanical quality factor Q and the chip temperature T. In addition, non-commuting terms lead to a disturbance via the measurement. First, there are the ones neglected as a result of the RWA, $H_{RWA} = \frac{1}{2}\omega_+''(0)x_{zp}^2(b^\dagger b^\dagger + bb)\hbar a^\dagger a$. Second, we consider terms due to a potential imprecise positioning that is not exactly at the avoided crossing $(x_0 \neq 0)$, $H_{lin} = \omega_+'(x_0)x_{zp}(b^\dagger + b)\hbar a^\dagger a$. The corresponding rates for measurement-induced transitions out of the ground state $\Gamma_{0\to n}$ are calculated using Fermi's golden rule; $\tau_{RWA}^{-1} = \Gamma_{0\to 2} = (\Delta\omega)^2 S_{NN}(-2\Omega)/2$, $\tau_{lin}^{-1} = \Gamma_{0\to 1} = (\omega_+'(x_0)x_{zp})^2 S_{NN}(-\Omega)$, where $S_{NN}(\omega) = \int \mathrm{d}t \exp(i\omega t)\langle N(t)N(0)\rangle$ with $N = a^\dagger a$. In a Pound-Drever-Hall scheme we have $S_{NN}(\omega) = (4P_{in}/\hbar\omega_c)/(\omega^2 + (\kappa/2)^2)$. Collecting all terms, we can calculate eq. (9).

For microwave setups with a small nanomechanical beam manufactured close to the central conductor of a stripline resonator, achieving optomechanical couplings $\epsilon \simeq 1$–$100\,\mathrm{kHz/nm}$ [13,23,25], the frequency shift per phonon $\Delta\omega \propto \epsilon^2$ turns out to be extremely small making Fock state detection impossible $(\Sigma \ll 1)$. A new on-chip

Table 1: Results on the signal-to-noise ratio Σ, eq. (9), for two sets of experimental parameters that would allow to observe an individual quantum jump from the mechanical ground state to the first excited state ($\Sigma \geqslant 1$). Further parameter $\omega_c/2\pi = 5\,\mathrm{GHz}$.

ϵ (MHz/nm)	m (pg)	$\Omega/2\pi$ (MHz)	$Q/10^5$	κ/Ω	$g/2\pi$ (MHz)	P_{in} (pW)	x_0 (pm)	n_{add}	T (mK)	Σ
65	10	11	3.5	1/70	0.5	200	0.5	1	20	1.0
70	10	11	5.0	1/100	0.5	50	0.5	1	20	1.2

microwave system however, consisting of an LC circuit where the plates of a parallel-plate condensator mechanically resonate, achieves $\epsilon = 65\,\mathrm{MHz/nm}$ [32]. Our proposal transfers to this scheme by stacking three such plates, see fig. 4(e). For experimentally realistic parameters [32], a calculation of Σ yields that a setup with this optomechanical coupling would allow to detect an individual quantum jump from the mechanical ground state to the first excited state, see table 1. Note that, in contrast to the setup discussed in [2], the parameters here are already in the small-splitting regime $g < \Omega$, and the details of Fock state detection in that regime may require further analysis. Finally, we point out that such a setup, even for $\Sigma < 1$, would allow one to measure "phonon shot noise", *i.e.* quantum energy fluctuations around an average phonon number, of a mechanically driven, ground-state–cooled mechanical oscillator [33].

Conclusion. – To conclude, we introduced and analyzed theoretically coupled multimode optomechanical systems for the microwave regime. In contrast to the optical domain, these systems possess coupling frequencies between the electromagnetic modes that are naturally in the range of typical mechanical frequencies ($g \simeq \Omega$). By calculating the transmission spectrum, we demonstrated how this allows one to manipulate the microwave field dynamics in terms of mechanical driving. In principle $g \simeq \Omega$ enables to realize all kinds of driven two- and multi-level dynamics known from quantum optics in the microwave light field. Our discussion mostly focussed on classical mechanical motion. However, for mechanical oscillators in the quantum regime, coupled multimode systems with $g \simeq \Omega$ will be particularly interesting. For instance it might be possible to realize hybridized states which are superpositions of states with a photon being in different modes and phonons in the mechanics. We furthermore proposed a multimode setup that allows coupling the microwave photon number to the square of mechanical displacement and enables QND Fock state detection. For experimentally realistic parameters we predicted the possibility to detect an individual quantum jump from the mechanical ground state to the first excited state. The same scheme also allows one to measure phonon shot noise. Both experiments would constitute a major breakthrough.

* * *

We acknowledge fruitful discussions with R. Gross, E. Weig, J. Teufel and K. Lehnert as well as support by the DFG (NIM, SFB 631, Emmy-Noether program), GIF and DIP.

REFERENCES

[1] Marquardt F. and Girvin S. M., *Physics*, **2** (2009) 40.
[2] Thompson J. D. *et al.*, *Nature*, **452** (2008) 72.
[3] Li M. *et al.*, *Nature*, **456** (2008) 480.
[4] Eichenfield M. *et al.*, *Nature*, **459** (2009) 550.
[5] Eichenfield M. *et al.*, *Nature*, **462** (2009) 78.
[6] Anetsberger G. *et al.*, *Nat. Phys.*, **5** (2009) 909.
[7] Heinrich G., Harris J. G. E. and Marquardt F., *Phys. Rev. A*, **81** (2010) 011801(R).
[8] Dobrindt J. M. and Kippenberg T. J., *Phys. Rev. Lett.*, **104** (2010) 033901.
[9] Sankey J. C. *et al.*, *Nat. Phys.*, **6** (2010) 707.
[10] Braginsky V. B., Vorontsov Y. I. and Thorne K. S., *Science*, **209** (1980) 547.
[11] Braginsky V. B., Khalili F. Y. and Thorne K. S., *Quantum Measurement* (Cambridge University Press) 1992.
[12] Jayich A. M. *et al.*, *New J. Phys.*, **10** (2008) 095008.
[13] Regal C. A., Teufel J. D. and Lehnert K. W., *Nat. Phys.*, **4** (2008) 555.
[14] Hertzberg J. B. *et al.*, *Nat. Phys.*, **6** (2010) 213.
[15] Knobel R. G. and Cleland A. N., *Nature*, **424** (2003) 291.
[16] LaHaye M. D. *et al.*, *Science*, **304** (2004) 74.
[17] Naik A. *et al.*, *Nature*, **443** (2006) 193.
[18] Etaki S. *et al.*, *Nat. Phys.*, **4** (2008) 785.
[19] Buks E. *et al.*, *EPL*, **81** (2008) 10001.
[20] Brown K. R. *et al.*, *Phys. Rev. Lett.*, **99** (2007) 137205.
[21] LaHaye M. D. *et al.*, *Nature*, **459** (2009) 960.
[22] O'Connell A. D. *et al.*, *Nature*, **464** (2010) 697.
[23] Teufel J. D. *et al.*, *Phys. Rev. Lett.*, **101** (2008) 197203.
[24] Teufel J. D., Regal C. A. and Lehnert K. W., *New J. Phys.*, **10** (2008) 095002.
[25] Rocheleau T. *et al.*, *Nature*, **463** (2010) 72.
[26] Teufel J. D. *et al.*, *Nat. Nanotechnol.*, **4** (2009) 820.
[27] Devoret M. H., *Quantum Fluctuations in Electrical Circuits,* in *Quantum Fluctuations: Les Houches Session LXIII, 1995* (Elsevier, Amsterdam) 1997, pp. 351–386, `http://adsabs.harvard.edu/abs/1997fqqf.conf..351D`.
[28] Blais A. *et al.*, *Phys. Rev. A*, **69** (2004) 062320.
[29] Unterreithmeier Q. P., Weig E. M. and Kotthaus J. P., *Nature*, **458** (2009) 1001.
[30] Eric D. and Black , *Am. J. Phys.*, **69** (2001) 79.
[31] Castellanos-Beltran M. A. *et al.*, *Nat. Phys.*, **4** (2008) 928.
[32] Teufel J. D. *et al.*, arXiv:1011.3067v1 preprint (2010).
[33] Clerk A., Marquardt F. and Harris J., *Phys. Rev. Lett.*, **104** (2010) 213603.